Available online at www.sciencedirect.com

ScienceDirect

journal homepage: www.elsevier.com/locate/dental

Influence of age-related changes on crack growth trajectories and toughening mechanisms in human dentin

*Ebrahim Maghami, Ahmad R. Najafi**

Department of Mechanical Engineering and Mechanics, Drexel University, 3141 Chestnut St., Philadelphia, PA 19104, USA

ARTICLE INFO

Article history:
Received 18 June 2022
Received in revised form
19 September 2022
Accepted 22 September 2022

Keywords:
Aged dentin
Occlusion
Dentinal tubules
Critical energy release rate
Phase field fracture

ABSTRACT

Objectives: Dentin microstructure undergoes changes with age and its materials properties degrade over time. In the present study, we investigate the coupled influence of increased filled tubules and decreased materials properties on the fracture behavior of human dentin.

Methods: We assume degraded materials properties are linked with increased advanced glycation end-products (AGEs) crosslinks in dentin tissue. We use morphological data of human molars to create 2D and 3D models of dentin microstructure, and utilize a phase field fracture framework to study crack growth trajectories. We construct aged dentin samples (i.e., filled tubules and degraded properties) and compare the fracture results with the samples without age-related changes.

Results: The simulations show an increase in the number of filled tubules can deactivate the toughening mechanisms such as crack deflection and microcracking. In addition, filled tubules have adverse impacts on the ability of peritubular dentin to shield microcracking. We further show how the dentinal tubules' orientations affect the crack surface growth. We also investigate that an increase in the AGEs level can result in increased brittleness.

Significance: The developed model and findings of the present study provide region-dependent information on crack growth trajectories as well as more understanding of crack surface growth at the presence of filled tubules.

1. Introduction

With aging, non-enzymatic advanced glycation end-products (AGEs) crosslinks can accumulate in human hard tissues such as dentin [1]. AGEs content is found in the intertubular collagenous matrix and within dentinal tubules of aged dentine [2]. It is suggested that AGEs accumulation can bring about morphological and mechanical changes in dentin [3]. Dentinal collagen can become more fragile and stiffer with the accumulation of AGEs and aging, which can also increase the fracture risk [2]. It is reported that the flexural strength of aged dentin with high AGEs levels is lower than that of young dentin, as examined for various regions [4].

* Corresponding author.
E-mail address: arn55@drexel.edu (A.R. Najafi).

https://doi.org/10.1016/j.dental.2022.09.009
0109-5641/

In addition to AGEs accumulation, another important change in dentin with age is the occlusion of tubules. Due to the continuous deposition of minerals with aging, the diameter of dentinal tubules gradually reduces, and consequently, the tubules are completely filled [5]. It is reported that aged dentin with a high density of filled tubules has a lower fracture toughness than young dentin [6]. It is also shown that the fracture surfaces of young and old dentin specimens after failure are not similar, and cracks can break peritubular dentin (PTDs) with ease in aged dentin [7].

Another important factor influencing the toughening mechanism in dentin is the orientation of the dentinal tubules [8]. In crack propagation parallel to the long axis of tubules, collagen fibrils and mainly uncracked ligaments are responsible for crack bridging [8]. However, such crack bridging mechanisms have not been recognized in crack growth perpendicular to the long axis of the tubules. Additionally, it is reported that the fracture toughness of the inner dentin layer is considerably less than that of the outer dentin layer. This is related to remarkable changes in the microstructural features from the outer layer to the inner layer [9]. For instance, the density and diameter of tubules increase and the PTDs thickness decrease from the outer to the inner dentin [10–12].

Such distinct features can change crack growth trajectory and affect toughening mechanisms in dentin microstructure. For example, tubules have essential impacts on major toughening mechanisms such as crack deflection and uncracked-ligament bridging [5,8]. However, these mechanisms become mostly inactive with aging due to an increase in the occlusion of tubules [6]. In addition, by conducting finite element simulations, Wang et al. [13] showed that PTD has an important role in shielding the formation of microcracks. In another study on local fracture around tubules by a damage plasticity model, it is indicated that the rate of microcracking in PTDs increases with a reduction in tubules' diameter and PTD thickness [14].

In the present study, we are interested in finding the combined influence of increased AGEs levels and filled tubules on the fracture behavior of human dentin. To do so, we report crack growth in the outer and inner layers of dentin. We also analyze the effect of tubules' orientations on crack propagation surface. To reach our purpose, we use a phase field fracture framework to simulate crack growth in dentin microstructure. The phase field method is a diffuse approach that is appropriate for simulating different crack growth trajectories such as crack branching, crack bridging, and merging [15]. The phase field framework also offers less numerical instability in handling crack initiation and propagation in comparison with discrete fracture methods [16,17]. Additionally, the phase field model presented in our study uses an energetic formulation to predict crack evolution during fracture processes and it does not incoperate no further criteria [18]. This diffuse method has been employed to analyze the fracture behavior of different materials such as human bone and dentin [19–22,23], brittle biomaterials [24], and polymeric nanocomposites [25].

2. Materials and methods

2.1. *Constructing finite element models of dentin microstructure*

2.1.1. *2D models*

To build the 2D models, we utilize the morphological information of inner and outer layers in human dentin investigated by Chu et al. [12]. The 2D models consist of dentinal tubules, PTD, and the intertubular matrix (ITD). Circular voids with diameter d_t are modeled as tubules and PTDs with thickness t_p surround the tubules as shown in Figs. 1 and 2. PTDs and tubules are then embedded in ITD and PTDs are perfectly bonded to the ITD matrix. Figs. 1 and 2 show the distribution of tubules for the models in inner and outer layers, respectively. Using the randomization procedure in MATLAB, tubules are placed in the ITD matrix. A minimum distance of 0.1 μm between PTDs is also assumed to prevent any intersections. We also consider a pre-crack (1.5 μm length) in the 2D models. The models' dimensions are 30 μm × 30 μm. The sizes of the tubules' diameter and PTD's thickness differ from the inner layer (d_t = 2 μm, t_p = 0.5 μm) to the outer one (d_t = 0.75 μm, t_p = 1.25 μm) [12].

To simulate the occlusion of dentinal tubules with age, we assume that the circular voids in the models are filled as depicted in Figs. 1 and 2. In the first step, we construct three different random 2D models for each region. As shown in Figs. 1 and 2, models R1, R2, and R3 are for the inner layer and models R4, R5, and R6 are for the outer layer. In the next step, we assume three cases for the percentage of occluded tubules such that 10 %, 30 %, and 50 %. The purpose of these three percentages is to show the increased occlusions with aging and compare their fracture behavior with the model that has 0 % occluded tubules.

2.1.2. *3D models*

Figure 3 illustrates the three-dimensional (3D) models of dentin microstructure, which have a uniform distribution with an equal distancing of tubules. As shown in Fig. 3, the tubules are extruded in four different directions to simulate four possible orientations of tubules with a pre-crack surface. The four orientations are anti-plane parallel (model R7), perpendicular (model R8), in-plane parallel (model R9), and inclined parallel (model R10).

In addition to the presented 3D models in Fig. 3, we build four other 3D models as shown in Fig. 4 that have different orientations for tubules (anti-plane parallel and perpendicular). The anti-plane parallel models are R11 and R12 and the perpendicular models are R13 and R14 in Fig. 4. In models R12 and R14, three tubules are filled to simulate occlusion of the tubules. Tubules are non-uniformly distributed with unequal distancing in the 3D models in Fig. 4.

All 3D models in the present study consist of sixteen tubules with d_t= 1.5 μm surrounded by PTDs with t_p = 0.5 μm. The dimensions of all 3D models are 12 μm × 12 μm × 12 μm. A pre-crack surface is cut in all models.

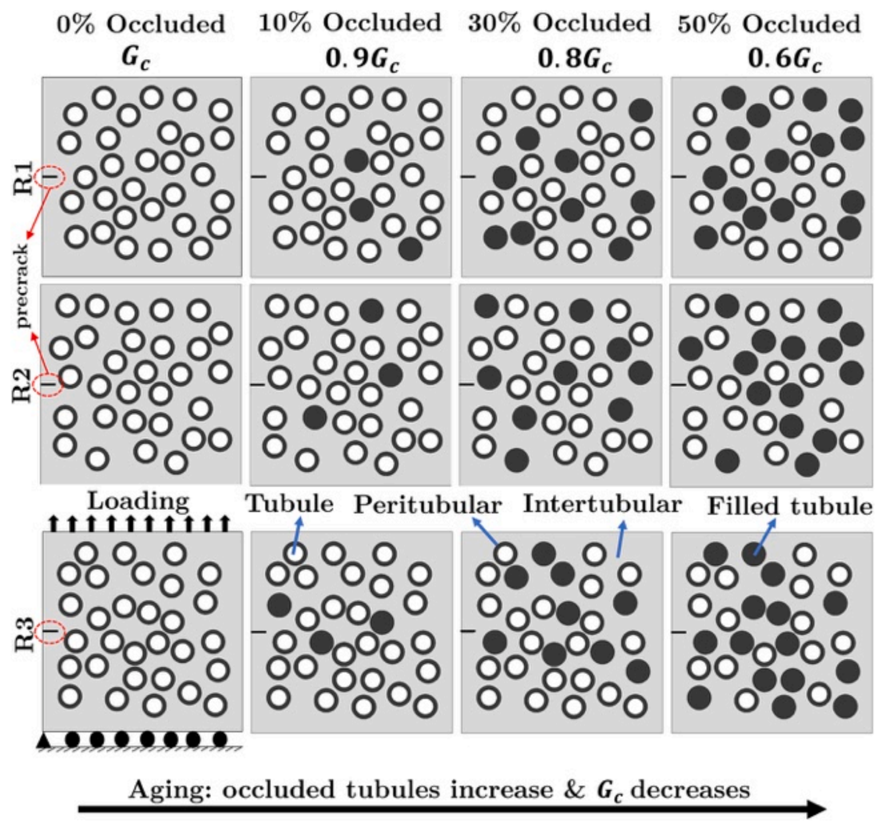

Fig. 1 – Three 2D models (R1, R2, and R3) representing the inner layer in dentin based on the morphological data investigated by Chu et al. [12]. The horizontal arrow shows the aging influence on dentin: increased occluded tubules and decreased energy release rates (G_c) of individual features (PTDs and ITD matrix). In all models, tubules are randomly distributed.

2.2. *The relationships between AGEs and G_c*

In human hard tissue like cortical bone, increased AGEs can lead to decreased energy release rate, G_c (a fracture property indicating the resistance to fracture) [26]. Dentin also has a similar composition to bone where AGEs can accumulate with age [4] and the aged dentin has a lower fracture toughness compared to the young dentin [27]. However, there is no clear data in the literature to show the relationship between elevated AGEs and G_c (or fracture toughness) in dentin. Based on the decrease in the fracture toughness and an increase in AGEs levels with age [4,27], we assume that increased AGEs in dentin with age can lead to a reduction in G_c and degrade its property in the present study. In addition to increased AGEs, another assumption is that the occlusion of tubules can change the crack growth trajectories and eventually result in a reduction in G_c. It should be noted that an increase in AGEs levels and occlusion of tubules can alter the elastic modulus of dentin. However, we do not include such changes in our study because changes in the elastic moduli do not affect the crack growth trajectories and it only alters the stress values.

2.3. *Mechanical properties of dentin microstructural features*

To simulate fracture in dentin, it is required to have the elastic moduli (E) and critical energy release rates (G_c) of PTD and ITD. As reported by experimental studies in the literature [28,29], the elastic moduli of the ITD and PTD are in the ranges of ~ 8–28 GPa and ~ 17–42 GPa, respectively. Here, we consider 12 GPa and 18 GPa as the elastic moduli of ITD and PTD, respectively. The Poisson's ratio for ITD and PTDs is assumed to be $\upsilon = 0.3$.

The fracture properties of the ITD matrix and PTD have not yet been reported in the literature. In the present study, we assume a ratio of 0.8 (G_{PTD}/G_{ITD}) between critical energy release rates of ITD (G_{PTD}) and PTD (G_{ITD}) based on suggestions proposed by An and Zhang [30]. Here, the ITD matrix is tougher than PTDs due to a high content of protein in the matrix [31,14,30]. We assume $G_{ITD} = 0.55\ N/mm$ based on calculations by $G = (1-\upsilon^2)K_c^2/E_{bulk}$ where $K_c = 3.4$ MPa. m$^{0.5}$ for the outer dentin layer reported by [9]. $E_{bulk} = 19$ GPa is the elastic modulus of the whole bulk of dentin [9]. We also consider all the materials are homogeneous and isotropic. We also assume that the filled tubules are stiffer (elastic modulus 10% more) but not tougher (Gc 10% less) than PTDs.

2.4. *Numerical simulation sets*

In the present study to evaluate the fracture behavior of dentin, we perform three sets of studies:

(I) In this set, we evaluate the combined influence of high AGEs levels and increased occlusions on the fracture

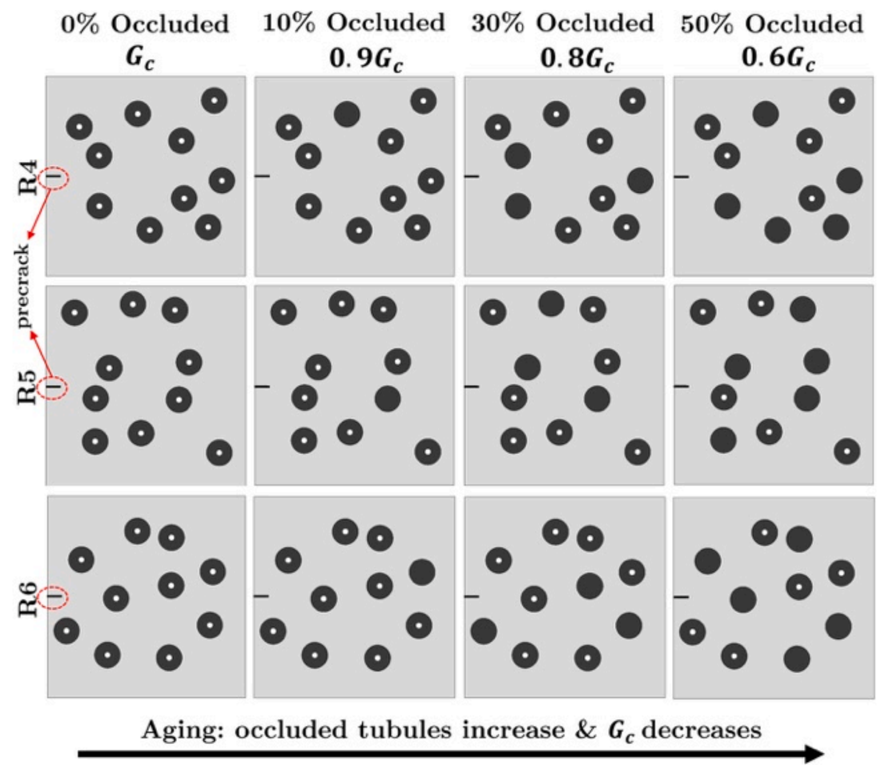

Fig. 2 – Three 2D models (R4, R5, and R6) representing the outer layer in dentin based on the morphological data investigated by Chu et al. [12]. The horizontal arrow shows the aging influence on dentin: increased occluded tubules and decreased energy release rates (G_c) of individual features (PTDs and ITD matrix). In all models, tubules are randomly distributed.

behavior of dentin (inner and outer layers). To reach this aim, we use the 2D models as presented in Sec. 2.1.1. We consider the filled tubules as occlusions: three cases for the percentage of occluded tubules such that 10 %, 30 %, and 50 % (Figs. 1 and 2). To simulate elevated AGEs levels in the models, we assume a 10 %, 20 %, and 40 % decrease in energy release rates of the ITD matrix and PTDs (G_{ITD}) and G_{ITD}) based on Sec. 2.2. To combine these two age-related changes, 10 %, 20 %, and 40 % decrease in G_{ITD} and G_{ITD} are assigned to 10%, 30%, and 50% increased occlusions, respectively. We apply this combination for all 2D models (R1 to R6). We compare the fracture results of these models with their reference models which have 0 % occlusions and no change in G_C. We also evaluate the effects of two factors (increased AGEs and increased occlusions) separately on the fracture behavior of dentin.

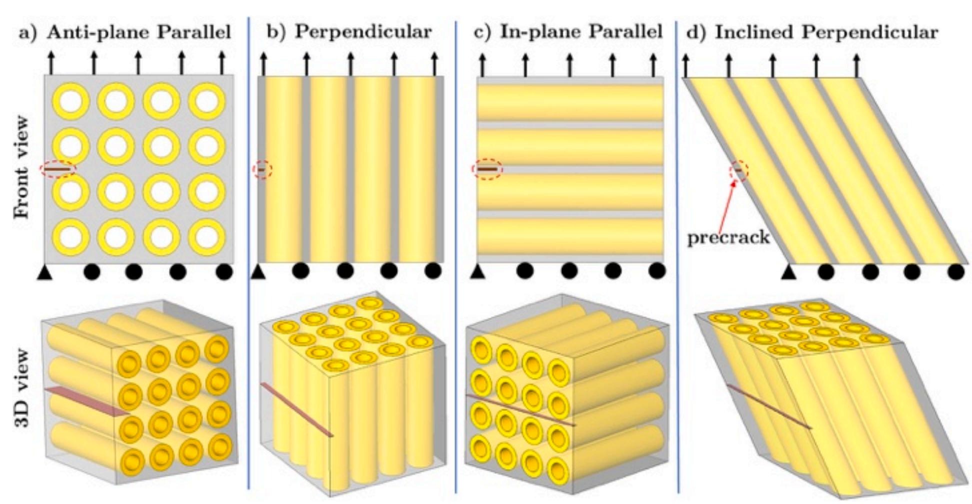

Fig. 3 – Four 3D models representing different directions that a crack surface can have with the tubules' orientations. In all models, tubules have the same uniform distribution.

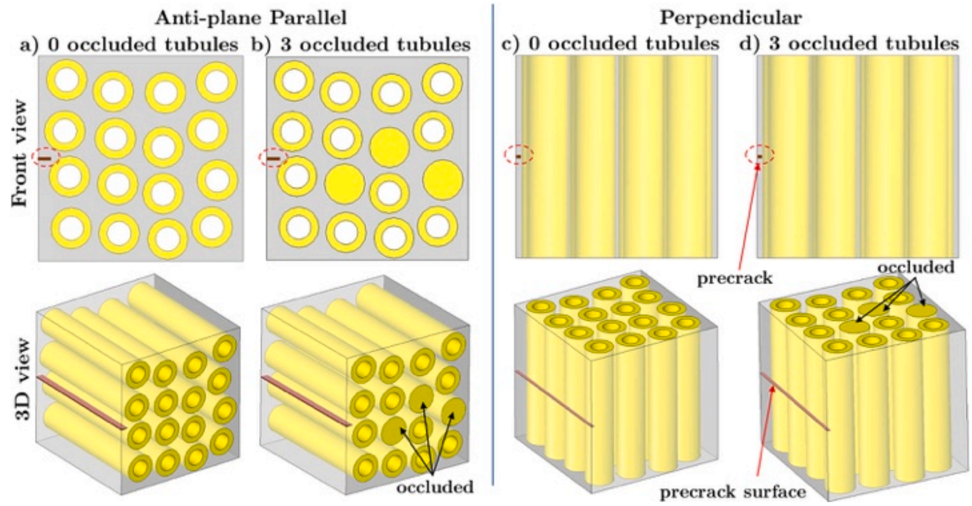

Fig. 4 – Two different tubules' orientations with a pre-crack surface in 3D models. The models with filled tubules represent as aged dentin microstructure with degraded energy release rates (G_c) of individual features (PTDs and ITD matrix). (a) and (c): tubules are not occluded. (b) and (d): three occluded tubules. In all models, tubules are randomly distributed.

(II) In the second set of studies, we investigate the influence of tubules' orientation on crack growth trajectories in dentin. To do so, we use the 3D models (R7 to R10) presented in Fig. 3 in Sec. 2.1.2. These models have a pre-crack surface and we apply a tensile loading as shown in Fig. 3. The results of this study report the possible reasons for different crack surfaces in the simulations from these models.

(III) In the third case of study, we analyze the crack growth in the 3D models with the random distribution of tubules as explained in Sec. 2.1.2 and shown in Fig. 4. These models have a pre-crack surface and we apply a tensile loading as shown in Fig. 4. G_c of models R12 and R14 (with some occlusions) are 10 % less than that of model R11 and R13 (with no occlusions). We compare the fracture results of the models with filled tubules (R12 and R14) with those of without occlusions (models R11 and R13). The aim is to understand how crack surface propagation in models R12 and R14 differs from that of models R11 and R13. Here, the results of these fracture simulations show two changes in dentin with age: decreased G_c (due to possible elevated AGEs) and increased occlusions.

2.5. *Phase field fracture framework*

To analyze the fracture behavior of dentin, we use a diffusive fracture framework presented by Miehe et al. [32]. In this framework, to simulate crack growth, we establish the minimization problem of an energy functional of a body such that

$$\Pi^{int} = E(\boldsymbol{u}, d) + W^{dmg}(d), \quad (1)$$

where Π^{int}, $E(\boldsymbol{u}, d)$, and $W^{dmg}(d)$ are the total potential energy, the elastic energy, and the required energy to form cracks, respectively. d introduces a damage field variable $d \in [0,1]$ where $d = 0$ and $d = 1$ describe the unbroken and broken material, respectively. $\boldsymbol{u}$ is the displacement field in the body.

The elastic energy in the damaged body takes the form

$$E(\boldsymbol{u}, d) = \int_{\Omega} \Psi(\varepsilon(\boldsymbol{u}), d)\, d\Omega, \quad (2)$$

where $\Psi(\varepsilon(\boldsymbol{u}), d)$ defines the strain energy density and $\varepsilon(\boldsymbol{u})$ is the symmetric strain tensor in the body. More details on the relationship between the stress tensor and the degraded strain energy can be found in the work of Miehe et al. [32].

The term of $W^{dmg}(d)$ in Eq. 1 forms such that

$$W^{dmg}(d) = \int_{\Omega} G_c\, \gamma(d, \nabla d)\, d\Omega, \quad (3)$$

where G_c is the critical energy release rate and $\gamma(d, \nabla d)$ is the crack density function defined by

$$\gamma(d, \nabla d) = \frac{1}{2l_c} d^2 + \frac{l_c}{2} \nabla d \,.\, \nabla d, \quad (4)$$

where l_c is the length scale parameter defining the damaged zone width between the unbroken and fully broken states of the material (the crack width) [33]. In the phase field approach, the diffusive crack is defined by the regularized crack surface function.

To solve the fracture problem, the energy functional for the phase field part takes the form

$$\Pi^{d} = \int_{\Omega} (G_c \gamma(d, \nabla d) + (1 - d^2)\, \mathscr{H}) d\Omega, \quad (5)$$

where $\mathscr{H}$ is strain history functional, which relates the displacement field to phase field and satisfies the irreversibility of the damage formation progress. We refer the readers for more details on the strain history functional to the work of Miehe et al. [32].

By having d variable from the previous functional, we establish the energy functional for the displacement field

$$\Pi^{u} \simeq E(\boldsymbol{u}, d) - W^{ext}, \quad (6)$$

where W^{ext} (the external work) forms by body forces and boundary tractions

$$W^{ext} = \int_{\Omega} \bar{\boldsymbol{b}}.\, \boldsymbol{u}\; d\Omega + \int_{\partial\Omega} \bar{\mathbf{t}}.\, \boldsymbol{u}\; d\partial\Omega, \quad (7)$$

where $\bar{\boldsymbol{b}}$ and $\bar{\mathbf{t}}$ are body forces and the boundary tractions, respectively. By substituting Eqs. 2 and 7 into Eq. 6, we obtain

$$\Pi^{u} = \int_{\Omega} (\Psi(\varepsilon(\boldsymbol{u}), d) - \bar{\boldsymbol{b}}.\, \boldsymbol{u})\; d\Omega - \int_{\partial\Omega} \bar{\mathbf{t}}.\, \boldsymbol{u}\; d\partial\Omega. \quad (8)$$

Having Eqs. 5 and 8, the strong forms for each field (the phase field and displacement) can be found by instructing the variations of the two energy functionals. More details on deriving the strong forms, the readers are referred to the studies by Miehe et al. [32] and Nguyen et al. [15].

We use a staggered scheme in a user-defined element subroutine (UEL) into Abaqus to solve the phase field and displacement problems suggested by Molnar and Gravouil [34]. More details on the finite element discretization are instructed based on the work of Molnar and Gravouil [34]. All 2D and 3D models contain four-node and hexagonal elements, respectively. The number of elements approximately are between ~ 200,000 and ~ 250,000 for 2D models and between ~ 3 million and ~ 3.2 million for 3D models. We also perform mesh convergence tests for all models. As presented in Fig. 1, we apply the tensile displacement loading on the top edge of 2D models (and surface for 3D models shown in Fig. 3) of the models. We use 1×10^{-6} mm increments for the first 400 steps and 1×10^{-7} mm increments for the remained steps to observe complete fracture in each model. As depicted in Fig. 1, we fix the bottom edge (surface for 3D models as presented in Fig. 3) along the y direction, and the bottom left corner (edge for 3D models) along the x and y directions. We also use the same length scale parameter in all simulations ($l_0 = 1.2 \times 10^{-4}$ mm) to present the thickness of the crack (presented in Eq. 4).

3. Results

To investigate the fracture behavior of dentin, we calculate the total absorbed energy (W^{tot}), damage initiation load (DIL), and crack length (or density). W^{tot} is the total toughness of the models until complete fracture. Figure 5 presents the fracture response of the random models (R1, R2, and R3) in the inner region of dentin. Here, we consider the models without filled tubules as healthy, and the models with filled tubules as aged samples with an increase in their AGEs level. Microcracking, crack deflection, and uncracked ligament bridging occur in our simulations on both healthy and aged models. One of the toughening mechanisms that frequently happens is the microcrack formation in PTDs. The rate of microcracking decreases and the fracture pattern alters with an increase in filled tubules. Our simulations also indicate that crack deflection is another important toughening mechanism. Tubules attract and deviates the main crack from its original path due to the high stress concentration of

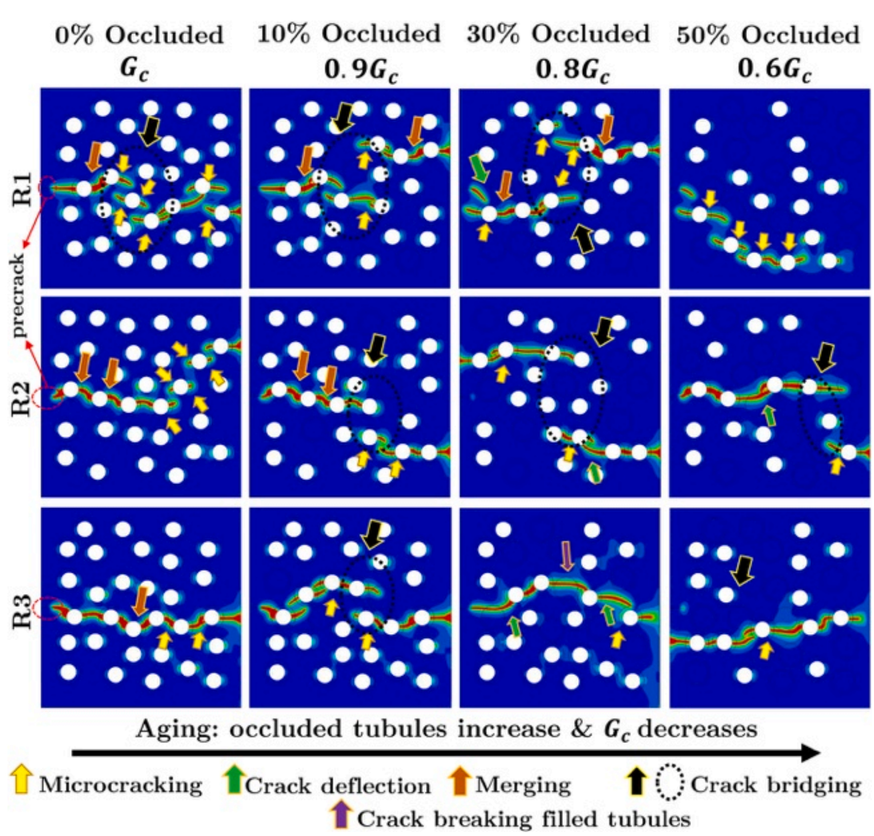

Fig. 5 – The fracture results of the presented 2D models (R1, R2, and R3) in Fig. 1. Microcracking decreases with an increase in filled tubules, forming relatively more straight cracks.

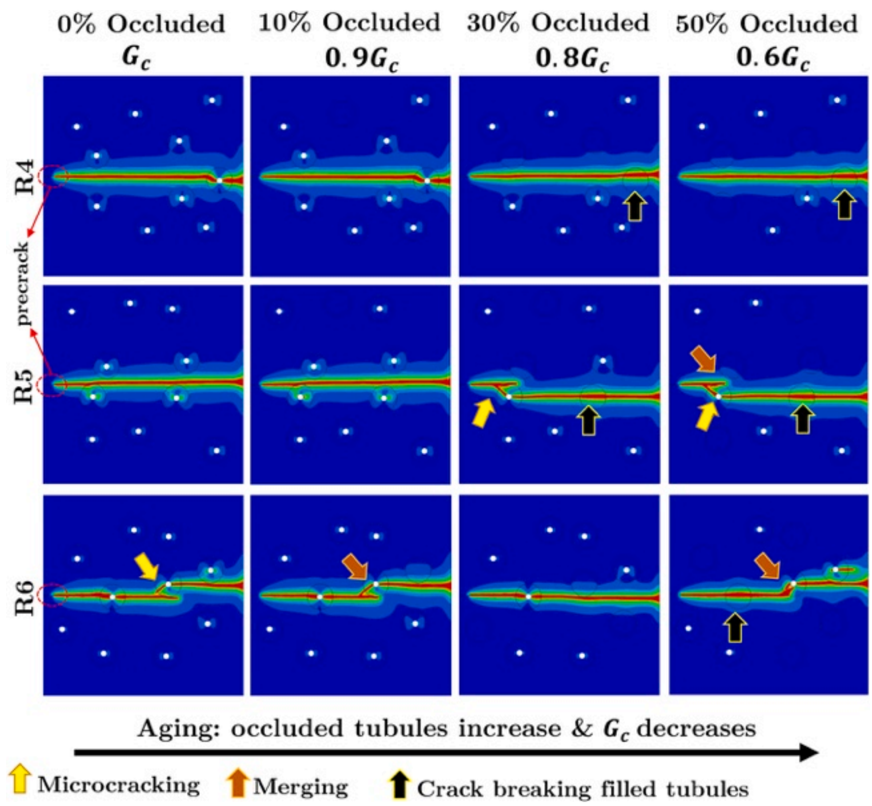

Fig. 6 – The fracture results of the presented 2D models (R4, R5, and R6) in Fig. 2. Cracks form in a more straight shape in the outer dentin region, and filled tubules have negligible impacts on cracks formations.

tubules. In the aged samples in the inner dentin region, the cracks deviate to the non-filled tubules.

Fig. 6 depicts the fracture behavior of the random models (R4, R5, and R6) in the outer region of dentin. The main crack in the outer models (both healthy and aged) initiates from the precrack and grows straightly without any significant deflection (Fig. 6). In addition, the cracks in the outer dentin mostly can break the filled tubules in aged samples. However, microcracks in the inner models (Fig. 5) can nucleate from tubules. This shows that there are more microcracks in the inner models than the outer models and in the outer dentin there are more long cracks.

We also calculate the energy absorption (the area under the curve) until the complete fracture for all aged and healthy models in both inner and outer dentin. With increased filled tubules and decrease in G_c (i.e., increase in AGEs level), the total energy absorption in models with filled decreases as well. Fig. 7 shows the decrease in the total energy of inner and outer models by increasing the filled tubules (10 %, 30 %, and 50 %) and reduced G_c. The DIL of models is also reduced with the combined influence of an increase in filled tubules and decreased G_c. In addition, cracks in the inner models initiate sooner than in the outer models (lower DIL in the inner models). This is in agreement with experiments where the resistance to crack initiation in inner dentin is lower than that of outer dentin [9]. Thus, the load for crack initiation in inner dentin is lower than that of outer dentin.

In addition, we investigate the influence of increased occlusions as a single factor on the fracture response of all 2D

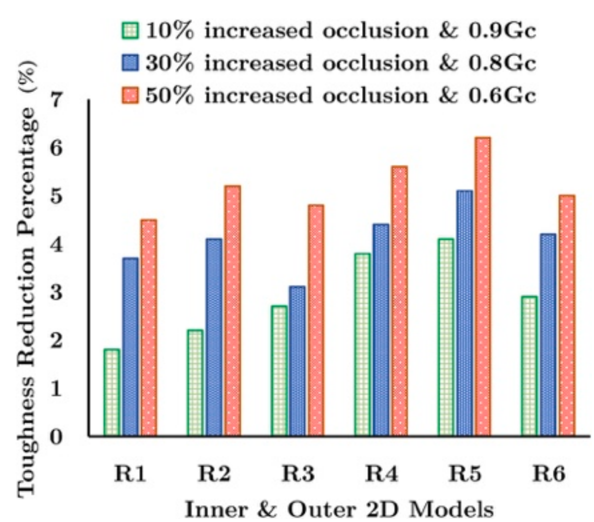

Fig. 7 – The decreased percentages in the total toughness value of each 2D model (R1, R2, R3, R4, R5, and R6) with respect to their initial model without filled tubules (0 % occlusion and Gc).

models (R1 to R6). For each model, we find that the patterns of crack growth trajectories of this case (considering the single factor of increased occlusions) are the same as the damage patterns in Figs. 5 and 6 for each scenario. However, there are some differences in their mechanical response from

0 % occlusions to 50 % for each model (force-displacement curve, post-yielding response). The reason for such differences is the different crack paths that are formed by adding more occlusions, which eventually alter the energy required to break the samples. We also evaluate the influence of the other individual factor, decreasing G_c due to increased AGEs, on the fracture response. If we only decrease the G_c of each 2D model without any filled tubules, the crack growth trajectories remain the same in that model (for each model similar to its initial case) because there are no changes in the proportion of fracture properties of ITD to PTD nor alterations in the geometrical features. However, the absorbed energy (W^{tot}) decreases with the reductions in the G_c values because G_c has a direct relationship with the absorbed energy. The decreased energy for each case of reduced G_c ($0.9G_c$, $0.8G_c$, and $0.6G_c$) in each model is nearly similar to those proportions presented in Fig. 7, with only a 4–5 % difference. These small differences are due to excluding the filled tubules.

Fig. 8 shows the influence of tubules' orientations on crack growth trajectories. In Fig. 8, we observe four cases of interactions between the crack surface and tubules' orientations. In the first case (anti-parallel), the crack surface nucleates from the precrack and then propagates toward the tubule ahead. Afterward, the crack surface breaks the tubules ahead without deflection. In the second case (perpendicular), the crack surface initiates from the precrack and breaks perpendicularly the entire tubule fibers. In the third case (in-plane parallel), damage nucleates from the precrack and gradually grows in the ITD matrix. But the crack surface deviates toward the tubules and propagates along the tubules' direction. In the last case (inclined perpendicular), the crack

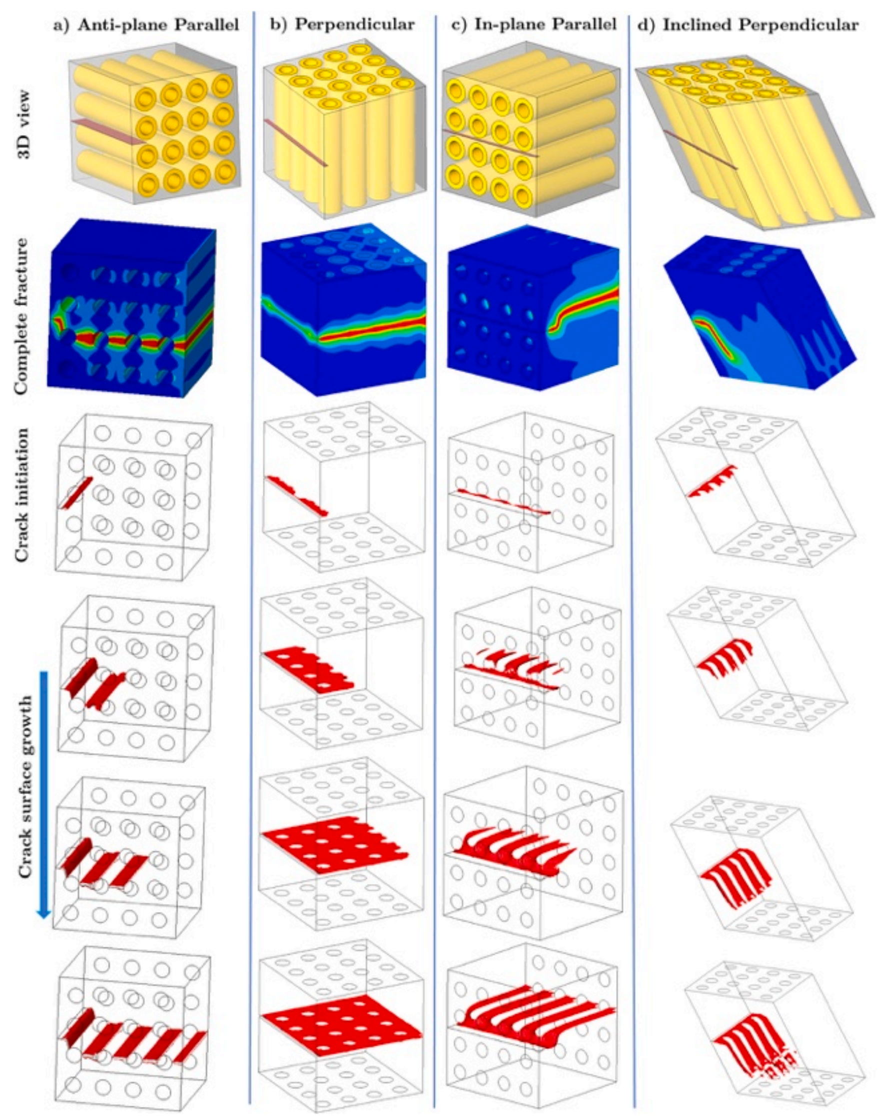

Fig. 8 – The fracture results for four 3D models presented in Fig. 3 different directions that a crack surface can have with the tubules' orientations. In all models, tubules have the same uniform distribution. In all simulations, the crack surface initiates from the precrack. Different tubules' orientations lead to different crack patterns.

surface forms from the precrack and breaks some inclined tubules. But it changes its direction and grows gradually along the inclined tubules.

The difference in fracture patterns and tubules' orientations in the 3D models cause different total toughness values. The ratios for the total toughness of perpendicular, in-plane parallel, and inclined perpendicular cases to that of the anti-plane parallel case are 0.82, 1.15, and 0.94, respectively.

Fig. 9 depicts fracture simulations of the 3D models with a random distribution of tubules. In Fig. 9, we observe how filled tubules can change the crack surface growth in the anti-plane parallel and perpendicular cases. In the anti-plane case without filled tubules (Fig. 9a), the crack surface initiates from the precrack and propagates to the adjacent tubule. In this model, microcracks also nucleate from other tubules and merge. In the anti-plane case with filled tubules (Fig. 9b), microcracks initiate from tubules and then merge and form the total crack surface. The crack surface density and the total toughness of the case with filled tubules (Fig. 9b) are 16 % greater and 20 % lower than those of the case without filled tubules (Fig. 9a), respectively.

As shown in Fig. 9c and d for the perpendicular mode, the crack surface grows perpendicular to the tubules' directions. In the case without filled tubules, damage initiates from the precrack. However, in the case with filled tubules (Fig. 9d), the crack initiates from inside of a filled tubule ahead of the precrack. In addition, the crack surface density and the total toughness of the case with filled tubules (Fig. 9d) are 5% greater and 12% lower than those of the case without filled tubules (Fig. 9c), respectively.

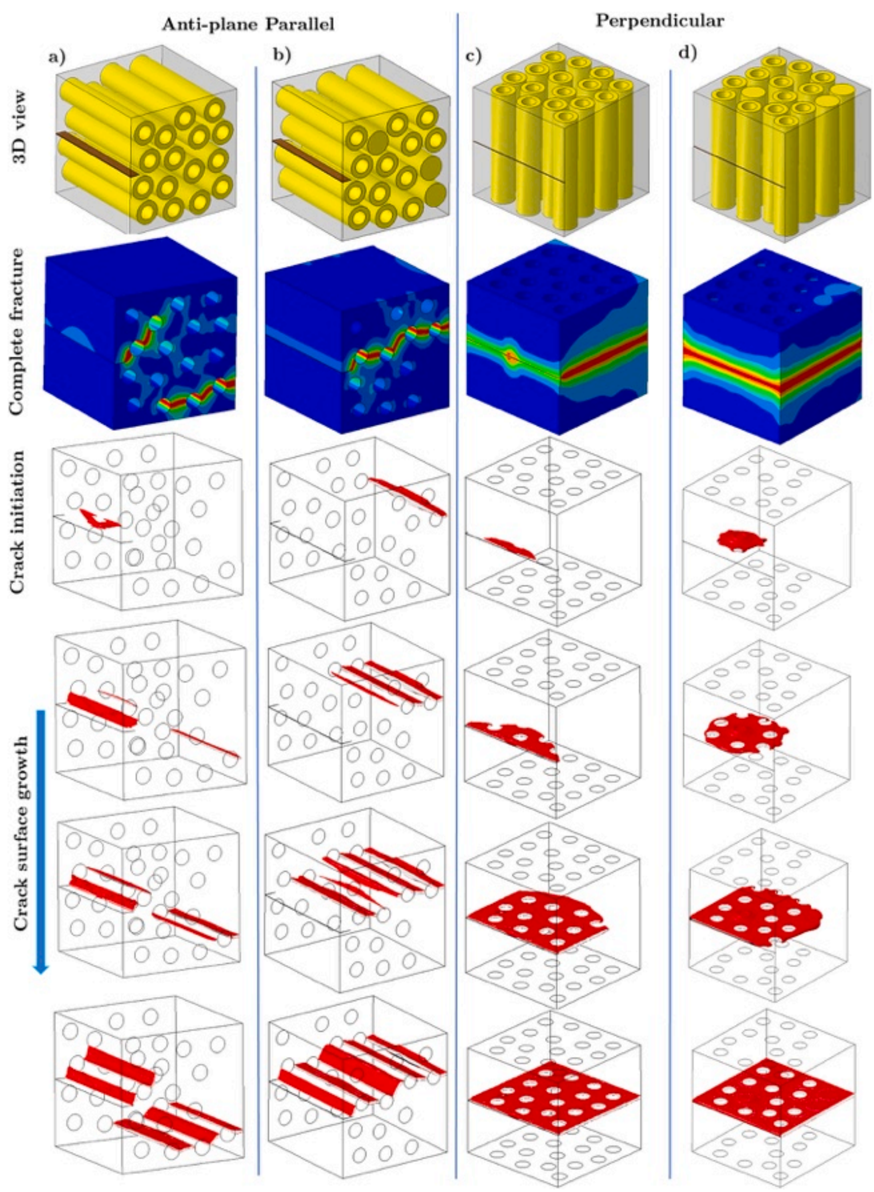

Fig. 9 – The fracture results for four 3D models are presented in Fig. 4. The filled tubules alter the crack surface growth in the anti-plane parallel case (compare (a) and (b)). Crack surface growth is perpendicular to the tubules' orientations in the perpendicular case (c and d). However, the crack surface initiations are different from (c) to (d).

4. Discussion

In the present study, we simulate the fracture behavior of dentin using a phase field fracture framework. Our aim is to investigate the coupled influence of increased filled tubules and decreased G_c on crack growth trajectory within dentin. We also evaluate the influence of these two factors individually on the fracture behavior of dentin microstructure. We consider two factors as aging factors in our study where we assume decreased G_c is linked to increased AGEs level in dentin based on the study conducted by Shinno et al. [4]. In the presented simulations, we also assume dentin as a fiber-reinforced material. In such a tissue, PTDs are hollow fibers and ITD is a matrix. The tubules are circular and cylindrical voids in our 2D and 3D simulations, respectively. With these assumptions, we can simulate a justifiable microstructure of dentin to investigate crack growth. To analyze the aging effects on crack growth trajectories, we evaluate the total energy absorption, the damage initiation load (DIL), and crack surface density for models with and without filled tubules.

One of the main toughening mechanisms observed in the dentin microstructure is PTD microcracking. Microcracking occurs occurred in both 2D and 3D models. In agreement with other studies [14,35,30], our results show that the presence of the tubules at the head of crack and microcracking in the tubules can control the crack propagation trajectory. The simulations also show that nucleated microcracks from tubules can merge and eventually form the main crack surface. In addition, the distribution of tubules can alter the main crack propagation. For instance, in the inner dentin region with a high density of tubules, microcracking in PTDs can result in uncracked ligament bridging and crack deflection, similar to experimental reports [5,9].

The microcracking, however, is affected by increased filled tubules. Our simulations show that an increase in filled tubules leads to a decrease in PTD microcracking. In addition, increased filled tubules can change cracks deflection. As indicated in Fig. 5, we observe that cracks are less deviated and tend to have a more likely straight formation in the inner dentin. Figure 5 also presents that cracks can break the filled tubules in some cases. Moreover, in the outer dentin as shown in Fig. 6, there are fewer microcracks than in the inner dentin models (Fig. 5). Cracks in the outer dentin models grow straightly with less deviation. Even with filled tubules, cracks still are in straight formations but some cracks can break the PTDs as well (Fig. 6). This shows that increased filled tubules have no influential impacts on crack growth trajectories in the outer dentin regions. The main reason for such straight cracks in the outer dentin (with or without filled tubules) is the low density of tubules in the outer dentin, which eventually result in less occurrence of cracks deviation. Another important factor to explain such crack growth trajectories can be also related to changes in material properties of dentin with aging. For instance, AGEs level increases with age and alters the collagen matrix of hard tissues such as dentin and bone [4,3,36]. With such an increase in AGEs levels, it is suggested that the glycated tissue becomes more fragile [36]. Thus, in brittle condition, cracks can have straight formations with no deflection.

It should be noted that tubules have an essential influence on important toughening mechanisms such as crack deflection and uncracked-ligament bridging [5,8]. However, with age-related changes in dentin microstructure such as the occlusion of tubules, these mechanisms become mostly inactive. Our simulations reveal this trend of inactivation which is in agreement with the study conducted by Montoya et al. [6]. In addition, PTDs can shield the propagation of microcracks [13,14]. However, with filled tubules, microcracking in PTDs decreases in dentin microstructure and there is a higher chance for a crack to propagate into the matrix. The influence of the increased AGEs and increased occlusions are also individually evaluated. The current simulations show that only decreasing Gc due to the increased AGEs can result in a reduction in the total absorbed energy (W^{tot}). This result is expected because reducing G_c of materials eventually causes decreased absorbed energy by the materials until the complete fracture. In addition, decreasing G_c as a single factor cannot change the crack growth pattern. The other factor, increasing the filled tubules, can result in changes in crack growth trajectories and some minor changes in the post-yielding response.

Another important factor in studying of crack growth trajectory in dentin is the tubules' orientations. Our 3D simulations show that the absorbed energy highly depends on the tubules' orientations. Here, in aged dentin, our results reveal that increased filled tubules can change the crack surface growth with respect to the tubules' orientations. In the antiplane parallel mode (Figs. 9a and b), our simulations show that filled tubules can entirely alter the crack surface pattern. However, in the perpendicular mode (Figs. 9c and d), the crack surface breaks all filled and non-filled tubules with a perpendicular angle. Increased filed tubules can also change the location of crack surface initiation in both 2D and 3D models.

Such information on crack growth trajectories in aged dentin is useful for the production of adhesives and bonding restorative materials to dentin. However, it should be noted in-depth investigations are still required for understanding micromechanics of fracture in aged dentin, and the present study has some limitations as well. The fracture properties of the PTD and ITD in the present study are based on the suggestions by other numerical studies [30,37], and these properties have not been yet experimentally characterized. It should be also noted that our simulations do not include the delamination at the interface between the PTD and ITD matrix, which is a toughening mechanism in dentin microstructure. Additionally, the length scale parameter l_c in the phase field method impacts the mechanical response, and experiments are required to investigate a suitable damage thickness for crack growth study in dentin microstructure. The morphological data for dentin microstructure differs from one tooth to another (density and diameters of tubules and PTDs thickness) [12]. In addition, the tubules' directions can have curvy formations from the outer surface of dentin to the inner surface, and the spacing between the tubules is not necessarily equal the same as the presented 3D models. Therefore, the results in the presented 2D and 3D models cannot be considered as dentin microstructure for all human teeth. Additionally, all inputs in our study have uncertain measurements. Therefore, uncertainty factors in such composite materials can influence the prediction of fracture patterns [38]. In the current study, it should be noted that there are differences between the size of the current simulations and those of the experimental specimens of dentin in the literature. Thus, for practical applications, it is not feasible to compare the mechanical response of the experiments in literature with the current simulations.

5. Conclusion

In the present study, we evaluate the influence of age-related changes (increased occluded tubules and degraded energy release rate) in dentin on crack growth trajectories. The main conclusions are

(i) Our results show that increased filled tubules can deactivate the toughening mechanisms such as crack deflection and microcracking.
(ii) The simulations indicate that cracks can break PTDs ahead in the models with filled tubules. In addition, the PTD shielding effect of microcracking is impaired in aged samples with filled tubules.
(iii) The filled tubules in the outer dentin models have minor impacts on crack growth trajectories.
(iv) Brittleness increases with degraded G_c property of dentin, which possibly can be related to elevated AGEs level.
(v) The 3D simulations show the crack surface and the crack density undergo changes with elevated filled tubules.
(vi) The phase-field fracture framework is a powerful numerical tool to investigate crack growth trajectories in dentin.

Conflict of interest

The authors declare that they have no conflict of interest.

Acknowledgments

The work is supported by the NSF CAREER Award CMMI-2143422. This work is also financed by the faculty start-up funding from the Department of Mechanical Engineering and Mechanics at Drexel University. The authors acknowledge the high-performance computing resources (Picotte: the Drexel Cluster) and support at Drexel University.

REFERENCES

[1] Alania Y, Trevelin LT, Hussain M, Zamperini CA, Mustafa G, Bedran-Russo AK. On the bulk biomechanical behavior of densely cross-linked dentin matrix: The role of induced-glycation, regional dentin sites and chemical inhibitor. J Mech Behav Biomed Mater 2020;103:103589.
[2] Miura J, Nishikawa K, Kubo M, Fukushima S, Hashimoto M, Takeshige F, et al. Accumulation of advanced glycation end-products in human dentine. Arch Oral Biol 2014;59(2):119–24.
[3] Ilea A, Băbţan AM, Boşca BA, Crişan M, Petrescu NB, Collino M, et al. Advanced glycation end products (ages) in oral pathology. Arch Oral Biol 2018;93:22–30.
[4] Shinno Y, Ishimoto T, Saito M, Uemura R, Arino M, Marumo K, et al. Comprehensive analyses of how tubule occlusion and advanced glycation end-products diminish strength of aged dentin. Sci Rep 2016;6(1):1–10.
[5] Koester KJ, Ager III JW, Ritchie RO. The effect of aging on crack-growth resistance and toughening mechanisms in human dentin. Biomaterials 2008;29(10):1318–28.
[6] Montoya C, Arola D, Ossa E. Importance of tubule density to the fracture toughness of dentin. Arch Oral Biol 2016;67:9–14.
[7] Arola D, Reprogel R. Effects of aging on the mechanical behavior of human dentin. Biomaterials 2005;26(18):4051–61.
[8] Nalla R, Kinney J, Ritchie R. Effect of orientation on the in vitro fracture toughness of dentin: the role of toughening mechanisms. Biomaterials 2003;24(22):3955–68.
[9] Ivancik J, Arola DD. The importance of microstructural variations on the fracture toughness of human dentin. Biomaterials 2013;34(4):864–74.
[10] Schilke R, Lisson JA, Bauß O, Geurtsen W. Comparison of the number and diameter of dentinal tubules in human and bovine dentine by scanning electron microscopic investigation. Arch Oral Biol 2000;45(5):355–61.
[11] Camargo CH, Siviero M, Camargo SEA, de Oliveira SH, Carvalho CA, Valera MC. Topographical, diametral, and quantitative analysis of dentin tubules in the root canals of human and bovine teeth. J Endod 2007;33(4):422–6.
[12] Chu CY, Kuo TC, Chang SF, Shyu YC, Lin CP. Comparison of the microstructure of crown and root dentin by a scanning electron microscopic study. J Dent Sci 2010;5(1):14–20.
[13] Wang R, Li Q, Niu L, Yang B, Liu G, Zuo H. Fracture toughening of peritubular microstructure in biological porous dentine. J Mech Behav Biomed Mater 2019;93:194–203.
[14] An B. Analysis of crack interacting with the composite microstructure of dentin. Eur J Mech A Solids 2017;66:287–95.
[15] Nguyen TT, Yvonnet J, Zhu QZ, Bornert M, Chateau C. A phase field method to simulate crack nucleation and propagation in strongly heterogeneous materials from direct imaging of their microstructure. Eng Fract Mech 2015;139:18–39.
[16] Mandal TK, Nguyen VP, Wu JY. Length scale and mesh bias sensitivity of phase-field models for brittle and cohesive fracture. Eng Fract Mech 2019;217:106532.
[17] Wu JY, Nguyen VP, Nguyen CT, Sutula D, Bordas S, Sinaie S. Phase field modeling of fracture. Adv Appl Mech 2018;52.
[18] Ambati M, Gerasimov T, De Lorenzis L. A review on phase-field models of brittle fracture and a new fast hybrid formulation. Comput Mech 2015;55(2):383–405.
[19] Maghami E, Moore JP, Josephson TO, Najafi AR. Damage analysis of human cortical bone under compressive and tensile loadings. Comput Methods Biomech Biomed Eng 2021:1–16.
[20] Josephson TO, Moore JP, Maghami E, Freeman TA, Najafi AR. Computational study of the mechanical influence of lacunae and perilacunar zones in cortical bone microcracking. J Mech Behav Biomed Mater 2022;126:105029.
[21] Maghami E, Pejman R, Najafi AR. Fracture micromechanics of human dentin: a microscale numerical model. J Mech Behav Biomed Mater 2021;114:104171.
[22] Maghami E, Josephson TO, Moore JP, Rezaee T, Freeman TA, Karim L, et al. Fracture behavior of human cortical bone: role of advanced glycation end-products and microstructural features. J Biomech 2021;125:110600.
[23] Nguyen L, Stoter S, Baum T, Kirschke J, Ruess M, Yosibash Z, et al. Phase-field boundary conditions for the voxel finite cell method: surface-free stress analysis of ct-based bone structures. Int J Numer Methods Biomed Eng 2017;33(12):e2880.

[24] Wu C, Fang J, Zhang Z, Entezari A, Sun G, Swain MV, et al. Fracture modeling of brittle biomaterials by the phase-field method. Eng Fract Mech 2020;224:106752.
[25] Msekh MA, Cuong N, Zi G, Areias P, Zhuang X, Rabczuk T. Fracture properties prediction of clay/epoxy nanocomposites with interphase zones using a phase field model. Eng Fract Mech 2018;188:287–99.
[26] Tang S, Vashishth D. The relative contributions of non-enzymatic glycation and cortical porosity on the fracture toughness of aging bone. J Biomech 2011;44(2):330–6.
[27] Nazari A, Bajaj D, Zhang D, Romberg E, Arola D. Aging and the reduction in fracture toughness of human dentin. J Mech Behav Biomed Mater 2009;2(5):550–9.
[28] Ziskind D, Hasday M, Cohen SR, Wagner HD. Young's modulus of peritubular and intertubular human dentin by nano-indentation tests. J Struct Biol 2011;174(1):23–30.
[29] Misra A, Spencer P, Marangos O, Wang Y, Katz JL. Micromechanical analysis of dentin/adhesive interface by the finite element method. J Biomed Mater Res Part B Appl Biomater 2004;70(1):56–65.
[30] An B, Zhang D. An analysis of crack growth in dentin at the microstructural scale. J Mech Behav Biomed Mater 2018;81:149–60.
[31] Xu C, Wang Y. Chemical composition and structure of peritubular and intertubular human dentine revisited. Arch Oral Biol 2012;57(4):383–91.
[32] Miehe C, Hofacker M, Welschinger F. A phase field model for rate-independent crack propagation: Robust algorithmic implementation based on operator splits. Comput Methods Appl Mech Eng 2010;199(45–48):2765–78.
[33] Bourdin B, Francfort GA, Marigo JJ. The variational approach to fracture. J Elast 2008;91(1–3):5–148.
[34] Molnár G. Gravouil A.2d and 3d abaqus implementation of a robust staggered phase-field solution for modeling brittle fracture. Finite Elem Anal Des 2017;130:27–38.
[35] An B, Xu Y, Zhang D. Crack initiation and propagation in composite microstructure of dentin. Int J Solids Struct 2017;110:36–43.
[36] Nyman JS. Effect of diabetes on the fracture resistance of bone. Clin Rev Bone Min Metab 2013;11(1):38–48.
[37] An B, Wagner HD. Role of microstructure on fracture of dentin. J Mech Behav Biomed Mater 2016;59:527–37.
[38] Hamdia KM, Silani M, Zhuang X, He P, Rabczuk T. Stochastic analysis of the fracture toughness of polymeric nanoparticle composites using polynomial chaos expansions. Int J Fract 2017;206(2):215–27.